



An analytic solution for blood flow in an artery with varying geometrical and mechanical properties

Olivier Delestre, Jose-Maria Fullana, Arthur R. Ghigo, Pierre-Yves Lagrée

► To cite this version:

Olivier Delestre, Jose-Maria Fullana, Arthur R. Ghigo, Pierre-Yves Lagrée. An analytic solution for blood flow in an artery with varying geometrical and mechanical properties. 2016. hal-01403335

HAL Id: hal-01403335

<https://hal.science/hal-01403335>

Preprint submitted on 1 Dec 2016

HAL is a multi-disciplinary open access archive for the deposit and dissemination of scientific research documents, whether they are published or not. The documents may come from teaching and research institutions in France or abroad, or from public or private research centers.

L'archive ouverte pluridisciplinaire **HAL**, est destinée au dépôt et à la diffusion de documents scientifiques de niveau recherche, publiés ou non, émanant des établissements d'enseignement et de recherche français ou étrangers, des laboratoires publics ou privés.

Olivier Delestre

Laboratoire J.A. Dieudonné, UMR CNRS 7351 & Polytech' Nice Sophia, University of Nice Sophia Antipolis (UNS)

Jose-Maria Fullana

Arthur R. Ghigo

Pierre-Yves Lagrée

Sorbonne Universités, CNRS and UPMC Université Paris 06, UMR 7190, Institut Jean Le Rond d'Alembert

An analytic solution for blood flow in an artery with varying geometrical and mechanical properties

Abstract

In this note, we present an analytic/exact solution of the one-dimensional model for blood flow. This solution describes the oscillation of a pulse wave in an artery with varying characteristics: cross-sectional area at rest and arterial wall rigidity. It is useful for the validation of numerical methods, especially well-balanced numerical methods.

arXiv - HAL

Contents

1	Introduction	3
2	Exact solution	3
3	Numerical experiments	6
4	Conclusion	6

1. Introduction

Large network blood flow simulations are performed using one-dimensional (1D) models that describe the conservation of mass and momentum in an artery. The 1D system of equations describing blood flow in the axial position x at time t writes:

$$\begin{cases} \frac{\partial A}{\partial t} + \frac{\partial Q}{\partial x} = 0 & (1a) \\ \frac{\partial Q}{\partial t} + \frac{\partial}{\partial x} \left[\frac{Q^2}{A} \right] + \frac{A}{\rho} \frac{\partial p}{\partial x} = S_f & (1b) \\ p = K [R - R_0], \quad K \in \mathbb{R}^{+*}. & (1c) \end{cases}$$

Using equation (1c), the momentum equation (1b) can be written as the momentum equation of a system of balance laws with source terms:

$$\frac{\partial Q}{\partial t} + \frac{\partial}{\partial x} \left[\frac{Q^2}{A} + \frac{K}{3\sqrt{\pi}\rho} A^{\frac{3}{2}} \right] = \frac{A}{\sqrt{\pi}\rho} \left[\frac{\partial}{\partial x} [K\sqrt{A_0}] - \frac{2}{3}\sqrt{A} \frac{\partial K}{\partial x} \right] + S_f. \quad (2)$$

The variables Q , A and P are respectively the flow rate, the cross-sectional area and the blood pressure. We also introduce the radius of the artery $R = \sqrt{A}/\sqrt{\pi}$ and the flow velocity $u = Q/A$. The variables R_0 , $A_0 = \pi R_0^2$ and K are respectively the radius at rest, the cross-sectional area at rest and the arterial wall rigidity. The parameter ρ is the density of blood and is supposed constant. The source term S_f represents the viscous friction term and will be described in the next section.

We propose an analytic solution of system (1) in an artery presenting an aneurysm (expansion of the radius at rest R_0). This solution can be used to validate numerical methods, especially well-balanced numerical methods [3, 6, 7, 2].

2. Exact solution

Inspired from the solutions of Thacker [11] and Sampson [10] well-known in the shallow water community, we look for a regular solution of system (1) rewritten in its nonconservative form:

$$\begin{cases} \frac{\partial}{\partial t} [\pi R^2] + \frac{\partial}{\partial x} [\pi R^2 u] = 0 & (3a) \\ \frac{\partial u}{\partial t} + u \frac{\partial u}{\partial x} + \frac{1}{\rho} \frac{\partial p}{\partial x} = S_f^*. & (3b) \end{cases}$$

The pressure p is given by equation (1c) and $S_f^* = S_f/A$, with:

$$S_f^* = -\bar{C}_f u, \quad \bar{C}_f \in \mathbb{R}^+. \quad (4)$$

Remark 1 Usually, the friction term of the nonconservative system (3) is $S_f^* = S_f/A = -[C_f/A] u$ with $C_f = 22\pi\nu$ [12]. The expression (4) can be seen as the linearization $-[C_f/A] u \simeq -[C_f/\bar{A}_0] u = -\bar{C}_f u$, where \bar{A}_0 is a reference constant cross-sectional area at rest.

Proposition 1 Assuming that the vector $[A, u]^T$ solution of system (3) is regular and that $u(x, t) = u_0(t)$, system (3) can be written as a single partial differential equation:

$$\frac{dF_0}{dt} - \rho u_0 \left[\frac{du_0}{dt} + \bar{C}_f u_0 \right] - \rho x \left[\frac{d^2 u_0}{dt^2} + \bar{C}_f \frac{du_0}{dt} \right] + K u_0 \frac{dR_0}{dx} - u_0 \frac{p}{K} \frac{dK}{dx} = 0, \quad (5)$$

where $F_0(t) \in \mathbb{R}$.

Proof. Considering that $u(x, t) = u_0(t)$ and that the solution is regular, we deduce from equation (3b) that:

$$p = F_0(t) - \rho x \left[\frac{du_0}{dt} + \bar{C}_f u_0 \right], \quad (6)$$

and then from equations (3a) and (1c) that:

$$\frac{1}{K} \frac{\partial p}{\partial t} + u_0 \left[\frac{\partial}{\partial x} \left[\frac{p}{K} \right] + \frac{dR_0}{dx} \right] = 0. \quad (7)$$

Injecting the expression (6) for p in equation (7), we obtain the expected result. \square

Remark 2 Equation (6) indicates that for each time t the pressure gradient is constant in space.

To describe aneurysms (expansions) as well as stenoses (constrictions), we choose the following spatial variations of the cross-sectional area at rest A_0 and of the arterial wall rigidity K in the domain $x \in [-a, a]$:

$$\begin{cases} R_0(x) = \bar{R}_0 \left[1 + \delta \left[1 - \frac{x^2}{a^2} \right] \right], & \bar{R}_0 > 0, \quad a > 0, \quad \delta > -1 \end{cases} \quad (8a)$$

$$\begin{cases} K(x) = \text{cst}, & K > 0. \end{cases} \quad (8b)$$

Injecting the expressions (8a) and (8b) in equation (5) and identifying the powers of x , we obtain the system of equations that will allow us to find an analytic solution for $(x, t) \in [-a, a] \times [0, +\infty]$:

$$\begin{cases} \frac{d^2 u_0}{dt^2} + \bar{C}_f \frac{du_0}{dt} + \delta \omega^2 u_0 = 0 \end{cases} \quad (9a)$$

$$\begin{cases} \frac{dF_0}{dt} - \rho u_0 \left[\frac{du_0}{dt} + \bar{C}_f u_0 \right] = 0. \end{cases} \quad (9b)$$

The parameter $\omega = 2c/a$ is the characteristic pulsation and $c = \sqrt{\frac{K}{2\rho} \bar{R}_0}$ is Moens-Korteweg celerity [9, 8].

Proposition 2 Under conditions:

$$0 < \delta \quad \text{and} \quad \bar{C}_f < 2\delta\omega, \quad (10)$$

and using the following initial and asymptotic viscous relaxation conditions:

$$u_0(t=0) = 0, \quad \lim_{t \rightarrow \infty} p(x, t) = 0, \quad (11)$$

the analytic solution of system (9) for $(x, t) \in [-a, a] \times [0, +\infty]$ is:

$$\begin{cases} u_0(t) = U \sin\left(\frac{t}{\tau}\right) e^{-\frac{\bar{C}_f}{2}t}, & U = \text{cst} \end{cases} \quad (12a)$$

$$\begin{cases} p(x, t) = -\frac{1}{2}\rho \frac{U^2}{\delta\omega^2\tau^2} H(\bar{C}_f, \tau, t)^2 - \rho x \frac{U}{\tau} H(\bar{C}_f, \tau, t), \end{cases} \quad (12b)$$

with

$$\tau = \frac{2}{\sqrt{|\bar{C}_f^2 - 4\delta\omega^2|}} \quad \text{and} \quad H(\bar{C}_f, \tau, t) = \left[\cos\left(\frac{t}{\tau}\right) + \frac{\bar{C}_f\tau}{2} \sin\left(\frac{t}{\tau}\right) \right] e^{-\frac{\bar{C}_f}{2}t}. \quad (13)$$

Remark 3 Conditions (10) describe an aneurysm (expansion) and naturally occur in physiological conditions as the pulsation $\omega \gg \bar{C}_f$ and $\delta = O(1)$.

Proof. The roots of the characteristic equation of the ordinary differential equation (9a) are:

$$\lambda_1 = -\frac{\bar{C}_f}{2} - \sqrt{s}, \quad \lambda_2 = -\frac{\bar{C}_f}{2} + \sqrt{s}, \quad (14)$$

with $s = [\bar{C}_f^2 - 4\delta\omega^2]/4 \in \mathbb{R}$. In the following, we note $\tau = 1/\sqrt{|s|}$ the characteristic time. Under conditions (10) the parameter $s < 0$. Using the initial condition (11), the solution of equation (9a) is then:

$$u_0 = U \sin\left(\frac{t}{\tau}\right) e^{-\frac{\bar{C}_f}{2}t}, \quad U = \text{cst}. \quad (15)$$

Injecting the solution (15) in equation (9b), we obtain:

$$F_0 = -\frac{1}{2}\rho \frac{U^2}{\delta\omega^2\tau^2} H(\bar{C}_f, \tau, t)^2 + C, \quad C = \text{cst}, \quad (16)$$

and finally we have:

$$p = -\frac{1}{2}\rho \frac{U^2}{\delta\omega^2\tau^2} H(\bar{C}_f, \tau, t)^2 - \rho x \frac{U}{\tau} H(\bar{C}_f, \tau, t) + C. \quad (17)$$

Using the asymptotic viscous relaxation condition (11) we have:

$$\lim_{t \rightarrow \infty} p = C = 0. \quad (18)$$

□

The final step is to specify the value of U . It must be chosen with respect to the following nonlinear stability arguments, namely that the radius R should remain positive:

$$R(x, t) > 0, \quad \forall (x, t) \in [-a, a] \times [0, +\infty], \quad (19)$$

and that the solution should not be discontinuous:

$$S_h^2(x, t) < 1, \quad \forall (x, t) \in [-a, a] \times [0, +\infty]. \quad (20)$$

The variable S_h is the Shapiro number (analogue of the Froude number for shallow water flows) and is defined as:

$$S_h^2(x, t) = \left[\frac{u_0(t)}{c(x, t)} \right]^2 = \left[\frac{u_0(t)}{\sqrt{\frac{K}{2\rho} R(x, t)}} \right]^2. \quad (21)$$

Proposition 3 *Under conditions (10), the inequalities (19) and (20) are true if the following sufficient condition is verified:*

$$|U| \leq \frac{1}{5} a \omega \left[\sqrt{5 + \delta} - \sqrt{\delta} \right]. \quad (22)$$

Proof. Using the pressure law (1c), we obtain the expression for the radius $R(x, t)$:

$$R(x, t) = \frac{\bar{R}_0 \delta}{a^2} \left[a^2 \frac{1 + \delta}{\delta} - \left[\frac{U}{\delta \omega^2 \tau} H(\bar{C}_f, \tau, t) \right]^2 - 2x \frac{U}{\delta \omega^2 \tau} H(\bar{C}_f, \tau, t) - x^2 \right]. \quad (23)$$

Under conditions (10), the function $R(x, t)$ is concave with respect to the variable x . Therefore two positions x_- and x_+ exist in which $R(x, t) = 0$ and are solutions of the following equation:

$$\left[x + \frac{U}{\delta \omega^2 \tau} H(\bar{C}_f, \tau, t) \right]^2 - a^2 \frac{1 + \delta}{\delta} = 0. \quad (24)$$

Noticing that:

$$\forall t \in [0, +\infty], \quad |H(\bar{C}_f, \tau, t)| \leq \sqrt{\delta \omega^2 \tau^2}, \quad (25)$$

we find the following upper and lower bounds of x_- and x_+ respectively:

$$x_- \leq \frac{|U|}{\sqrt{\delta} \omega} - a \sqrt{\frac{1 + \delta}{\delta}}, \quad x_+ \geq -\frac{|U|}{\sqrt{\delta} \omega} + a \sqrt{\frac{1 + \delta}{\delta}}. \quad (26)$$

The condition (19) is true if $(x_-, x_+) \notin [-a, a]^2$. Therefore a sufficient condition is:

$$|U| \leq a \omega \left[\sqrt{1 + \delta} - \sqrt{\delta} \right] \quad (27)$$

Under the condition (27), the minimum $R_{min}(t)$ of $R(x, t)$ for $x \in [-a, a]$ is reached in either $x = -a$ or $x = a$. Using the inequality (25), we find the following lower bound of $R_{min}(t)$:

$$R_{min}(t) \geq \bar{R}_0 \left[1 - \left[\frac{U}{a \omega} \right]^2 - 2\sqrt{\delta} \frac{|U|}{a \omega} \right] > 0. \quad (28)$$

Noticing that:

$$\forall t \in [0, +\infty], \quad |u_0(t)| \leq |U|, \quad (29)$$

and using the inequality (28), we obtain the following upper bound for $S_h(x, t)$:

$$S_h(x, t)^2 \leq \frac{4U^2}{\left[a^2 \omega^2 - U^2 - 2\sqrt{\delta} a \omega |U| \right]}. \quad (30)$$

To satisfy the inequality (20), a sufficient condition is that:

$$5U^2 + 2\sqrt{\delta} a \omega |U| - a^2 \omega^2 \leq 0. \quad (31)$$

Calculations allow us to show that the inequality (31) is verified if:

$$|U| \leq \frac{1}{5} a \omega \left[\sqrt{5 + \delta} - \sqrt{\delta} \right]. \quad (32)$$

As $\min \left(\sqrt{1 + \delta} - \sqrt{\delta}, \frac{1}{5} \left[\sqrt{5 + \delta} - \sqrt{\delta} \right] \right) = \frac{1}{5} \left[\sqrt{5 + \delta} - \sqrt{\delta} \right]$ for $\delta > 0$, this concludes the proof. \square

3. Numerical experiments

We now compare the analytic solution (12) to the results of a finite volume well-balanced numerical scheme. For details on the numerical method, we refer the reader to [13, 5, 4, 1]. The parameters of the simulation are presented in table 1 and are representative of averaged physiological flow conditions in large arteries. Furthermore, they are chosen such that the conditions (10) and (22) are satisfied. The simulations are performed using $N = 100$ cells of equal size and a time step $\Delta t = 1 \times 10^{-4}$.

ρ [$g.cm^{-3}$]	\bar{R}_0 [cm]	a [cm]	δ [cm]	K [$g.cm^{-2}.s^{-2}$]	\bar{C}_f [s^{-1}]	U [$cm.s^{-1}$]	c [$cm.s^{-1}$]	ω [s^{-1}]	τ [s]
1	1	4	$\frac{1}{4}$	1×10^4	5	1	100	50	4.02×10^{-2}

Table 1: Geometrical and mechanical parameters describing the artery, given in "cgs".

In figure 1, we plot the spacial evolution of the velocity $u_0(t)$, of the flow rate $Q(x, t)$ and of the pressure $p(x, t)$ at five different times $\{t_1 = 0.05, t_2 = 0.2, t_3 = 0.4, t_4 = 0.6, t_5 = 0.9\}$ s. At each time t and for each quantity, we observe a good agreement between the analytic and the numerical solutions.

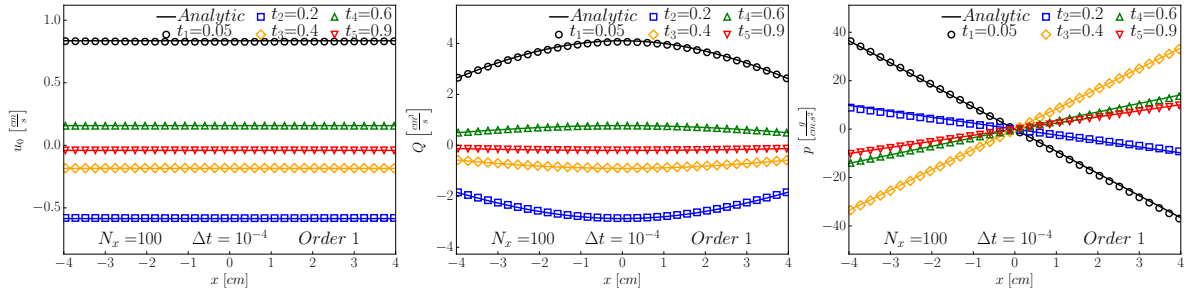


Figure 1: Comparison between the analytic (—) and the numerical solutions (marks) for the velocity $u_0(t)$, the flow rate $Q(x, t)$ and the pressure $p(x, t)$ at five different times $t = \{t_1 = 0.05, t_2 = 0.2, t_3 = 0.4, t_4 = 0.6, t_5 = 0.9\}$ s. We observe a good agreement between the analytic and numerical solutions for each quantity at every time.

In figure 2, we plot the temporal evolution of the velocity $u_0(t)$, of the flow rate $Q(x, t)$ and of the pressure $p(x, t)$ at three different positions $x = \{x_1 = -a/2, x_2 = 0, x_3 = +a/2\}$. At each position x and for each quantity, we observe a good agreement between the analytic and the numerical solutions.

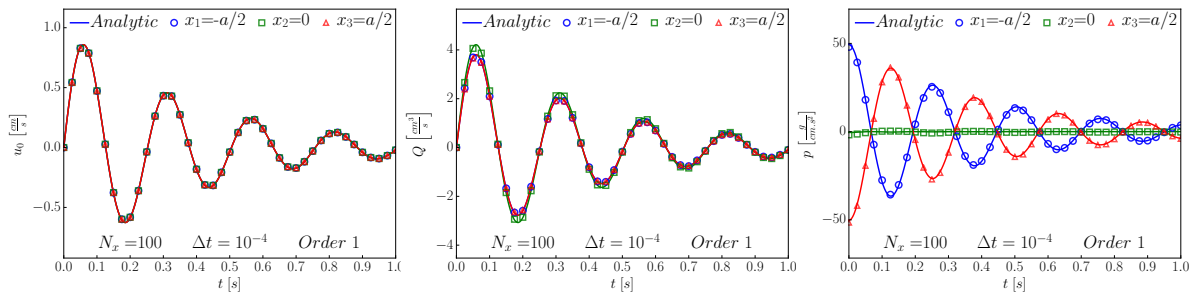


Figure 2: Comparison between the analytic (—) and the numerical solutions (marks) for the velocity $u_0(t)$, the flow rate $Q(x, t)$ and the pressure $p(x, t)$ at three different positions $x = \{x_1 = -a/2, x_2 = 0, x_3 = +a/2\}$. We observe a good agreement between the analytic and numerical solutions for each quantity at every position.

4. Conclusion

We have presented a viscous analytic solution of system (3) in an aneurysm. This solution describes the long-wave oscillations and viscous dissipation of the pressure pulse inside the aneurysm. We found good agreement between this analytic solution and the numerical solution obtained using a finite volume well-balanced

numerical scheme, indicating that this analytic solution can be used to validate numerical schemes in arteries with aneurysms.

References

- [1] Chloe Audebert, Petru Bucur, Mohamed Bekheit, Eric Vibert, Irene E Vignon-Clementel, and Jean-Frédéric Gerbeau. Kinetic scheme for arterial and venous blood flow, and application to partial hepatectomy modeling. *Computer Methods in Applied Mechanics and Engineering*, 2016.
- [2] Emmanuel Audusse, François Bouchut, Marie-Odile Bristeau, Rupert Klein, and Benoît Perthame. A fast and stable well-balanced scheme with hydrostatic reconstruction for shallow water flows. *SIAM Journal on Scientific Computing*, 25(6):2050–2065, 2004.
- [3] Alfredo Bermúdez and Ma Elena Vázquez. Upwind methods for hyperbolic conservation laws with source terms. *Computers & Fluids*, 23(8):1049–1071, 1994.
- [4] Olivier Delestre, Arthur R Ghigo, J-M Fullana, and P-Y Lagrée. A shallow water with variable pressure model for blood flow simulation. *Networks and Heterogeneous Media*, 11(1):69–87, 2016.
- [5] Olivier Delestre and P-Y Lagrée. A well-balanced finite volume scheme for blood flow simulation. *International Journal for Numerical Methods in Fluids*, 72(2):177–205, 2012.
- [6] Laurent Gosse and Alain-Yves LeRoux. Un schéma-équilibre adapté aux lois de conservation scalaires non-homogènes. *CR Acad. Sci. Paris Sér. I Math*, 323(5):543–546, 1996.
- [7] Joshua M Greenberg and Alain-Yves LeRoux. A well-balanced scheme for the numerical processing of source terms in hyperbolic equations. *SIAM Journal on Numerical Analysis*, 33(1):1–16, 1996.
- [8] DJ Korteweg. Über die fortpflanzungsgeschwindigkeit des schalles in elastischen röhren. *Annalen der Physik*, 241(12):525–542, 1878.
- [9] A Isebre Moens. *Die pulskurve*. EJ Brill, 1878.
- [10] Joe Sampson, Alan Easton, and Manmohan Singh. Moving boundary shallow water flow above parabolic bottom topography. *Anziam Journal*, 47:373–387, 2006.
- [11] William Carlisle Thacker. Some exact solutions to the nonlinear shallow-water wave equations. *Journal of Fluid Mechanics*, 107:499–508, 1981.
- [12] Xiao-Fei Wang, Shohei Nishi, Mami Matsukawa, Arthur Ghigo, Pierre-Yves Lagrée, and Jose-Maria Fullana. Fluid friction and wall viscosity of the 1d blood flow model. *Journal of biomechanics*, 49(4):565–571, 2016.
- [13] Xiaofei Wang, Jose-Maria Fullana, and Pierre-Yves Lagrée. Verification and comparison of four numerical schemes for a 1D viscoelastic blood flow model. *Computer methods in biomechanics and biomedical engineering*, 18(15):1704–1725, 2015.